TABLE 2-II Continued

TEST	FREQUENCY (Hz)	AMPLITUDE (in)	PEAK VELOCITY (in/sec)	PEAK FORCE (lb)	DISSIPATED ENERGY (lb-in)	STORAGE STIFFNESS (lb/in)	LOSS STIFFNESS (lb/in)	DAMPING COEFFICIENT (lb-sec/in)	PHASE ANGLE (degrees)	TEMPERATURE (°C)
22	2.0	0.26	3.242	308.7	225.5	0	1078.3	85.8	90	23
23	2.0	0.26	3.217	312.0	220.2	0	1069.5	85.1	90	23
24	2.0	0.26	3.242	282.2	213.6	0	1021.4	81.3	90	23
25	2.0	0.26	3.217	332.3	224.2	0	1088.9	86.7	90	23
26	2.0	0.26	3.242	328.3	240.0	0	1147.7	91.3	90	22
27	2.0	0.26	3.230	489.6	292.0	0	1407.2	112.0	90	2
28	2.0	0.26	3.230	224.6	178.2	0	858.8	68.3	90	46
29	2.0	0.51	6.434	587.6	886.6	0	1076.6	85.7	90	23
30	2.0	0.51	6.421	624.0	943.9	0	1150.6	91.6	90	23
31	2.0	0.51	6.434	896.0	1245.7	0	1512.6	120.4	90	2
32	2.0	0.52	6.472	551.0	851.4	0	1021.8	81.3	90	23
33	2.0	1.02	12.818	1083.0	3472.2	0	1062.3	84.5	90	23
34	2.0	1.02	12.818	1136.5	3638.9	0	1113.3	88.6	90	23
35	2.0	1.03	12.943	1083.0	3415.7	0	1024.8	81.6	90	23
36	2.0	1.03	12.943	1488.0	4754.3	0	1426.5	113.5	90	1
37	4.0	0.26	6.434	597.5	443.3	444.4	2153.1	85.7	79.0	23
38	4.0	0.26	6.434	864.0	571.0	773.0	2773.3	110.3	76.8	2
39	4.0	0.26	6.434	624.6	439.1	492.3	2132.7	84.9	78.3	23
40	4.0	0.51	12.918	1182.7	1811.0	423.0	2181.9	86.8	79.4	23
41	4.0	0.51	12.893	1175.0	1824.5	612.1	2206.8	87.8	74.5	23
42	4.0	0.52	12.994	1120.3	1744.4	416.7	2077.4	82.7	78.9	23

TABLE 2-II Continued

TEST	FREQUENCY (Hz)	AMPLITUDE (in)	PEAK VELOCITY (in/sec)	PEAK FORCE (lb)	DISSIPATED ENERGY (lb-in)	STORAGE STIFFNESS (lb/in)	LOSS STIFFNESS (lb/in)	DAMPING COEFFICIENT (lb-sec/in)	PHASE ANGLE (degrees)	TEMPERATURE (°C)
43	4.0	0.52	12.969	995.9	1600.0	333.3	1912.8	76.1	80.1	23
44	4.0	0.52	13.044	1552.0	2419.3	640.0	2858.9	113.8	77.6	2
45	4.0	0.52	12.943	858.3	1373.3	246.3	1648.2	65.6	81.5	47
46	6.0	0.10	3.597	345.6	86.1	798.6	3011.3	79.9	77.3	25
47	6.0	0.44	16.738	1840.0	2470.3	1000.0	3988.7	105.8	67.3	2
48	6.0	0.47	17.530	1410.8	2036.6	666.7	2998.1	79.5	77.3	23
49	6.0	0.48	18.209	1538.5	2297.6	707.8	3134.9	83.2	77.2	23
50	8.0	0.10	4.785	451.2	114.6	1284.0	4025.0	80.1	74.3	25
51	8.0	0.26	12.818	1095.4	757.3	1250.0	3707.1	73.8	73.0	23
52	8.0	0.26	12.969	1045.6	801.8	1312.7	3834.2	76.3	71.1	23
53	8.0	0.26	12.818	1153.8	795.4	1307.7	3893.6	77.5	73.2	24
54	20.0	0.04	5.027	385.2	35.6	6530.7	7082.4	56.4	47.3	27
55	20.0	0.05	6.522	535.4	63.9	6365.3	7551.2	60.1	51.9	23
56	20.0	0.08	10.430	876.0	192.6	5670.8	8899.2	70.8	57.5	27
57	25.0	0.04	6.707	521.8	47.3	9008.0	8257.6	52.6	40.4	23
58	25.0	0.07	11.357	921.9	164.8	8328.5	10035.3	63.9	49.2	23

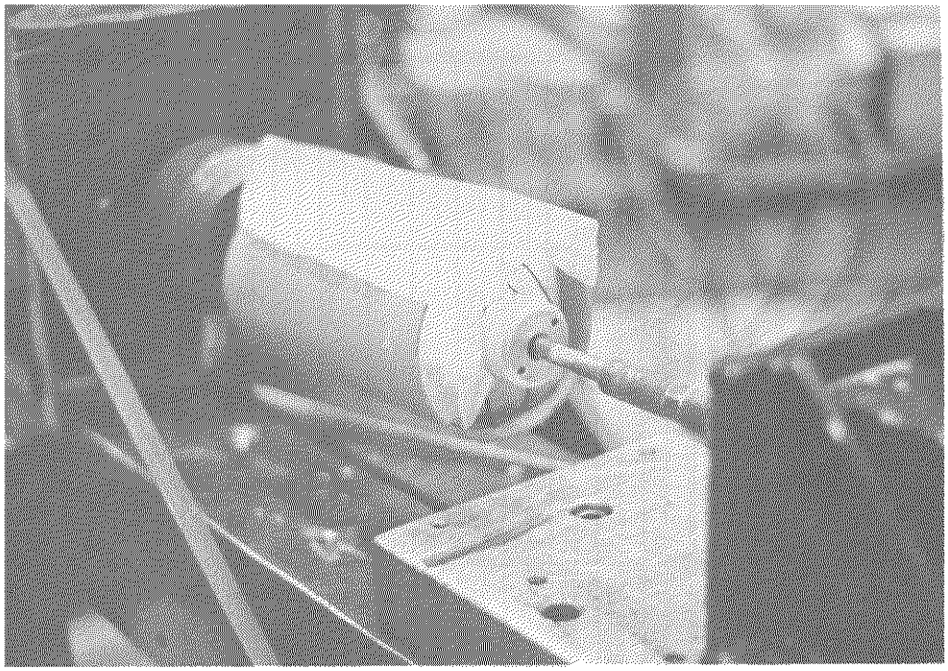

FIGURE 2-5 **View of Testing Arrangement in Low Temperature Tests**

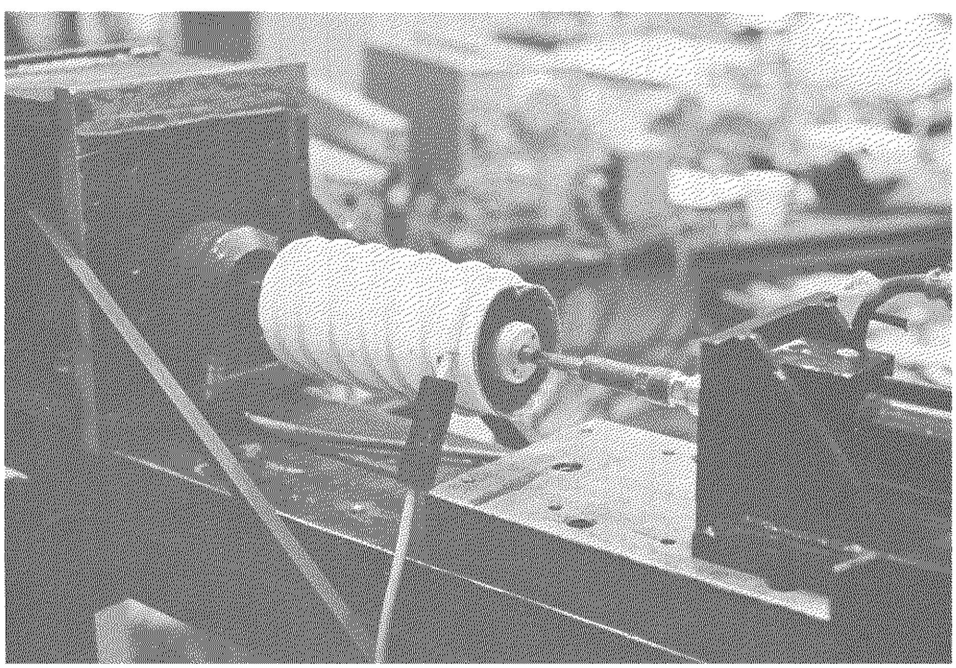

FIGURE 2-6 **View of Testing Arrangement in High Temperature Tests**

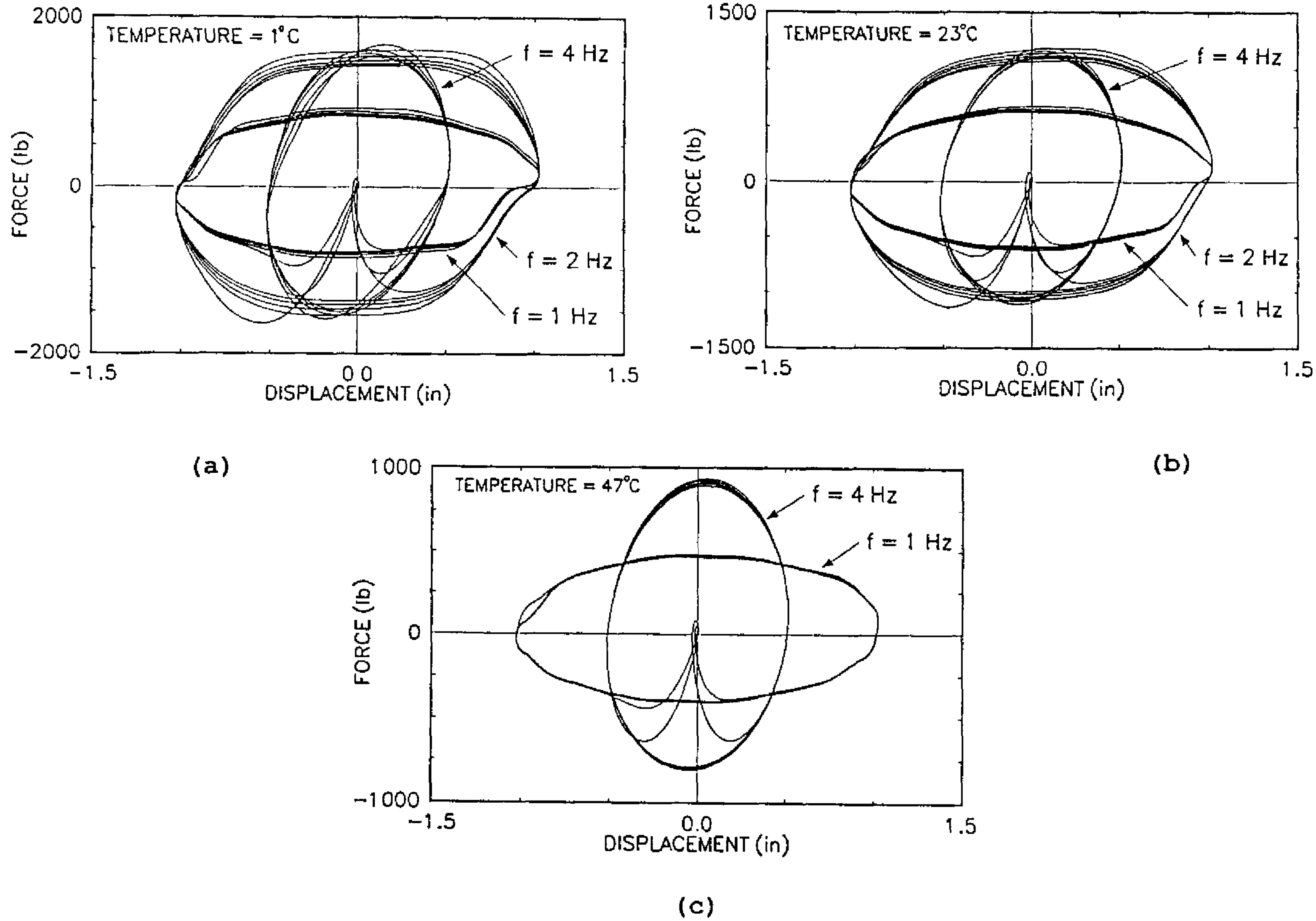

FIGURE 2-7 **Recorded Force - Displacement Loops at (a) Low Temperature, (b) Room Temperature, and (c) High Temperature (1 in. = 25.4 mm, 1 lb = 4.46 N)**

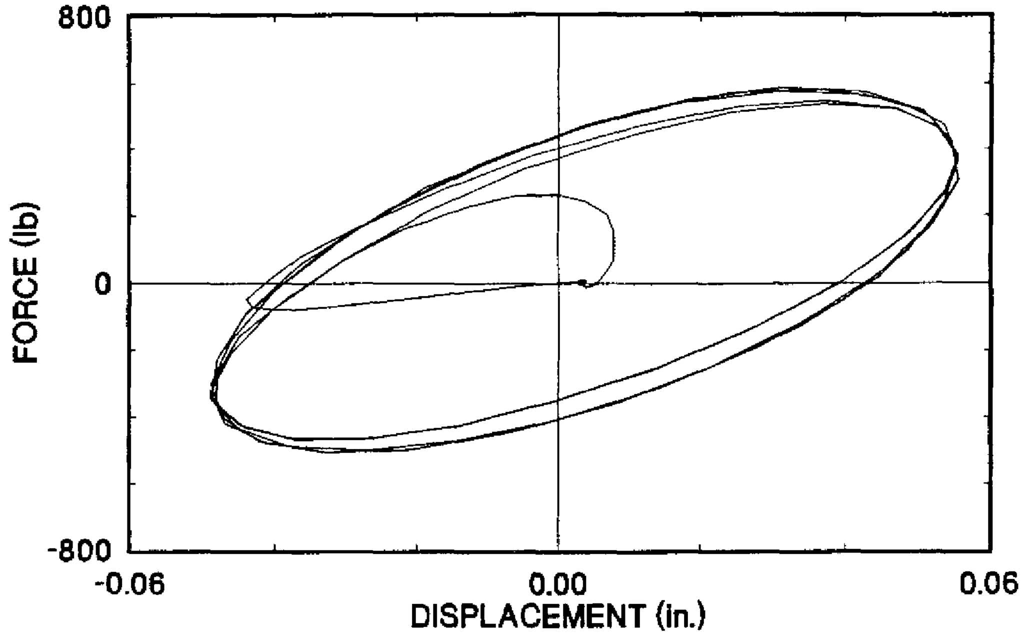

FIGURE 2-8 Recorded Force - Displacement Loop at Frequency of 20 Hz and Temperature of 23°C (1 in. = 25.4 mm, 1 lb = 4.46 N)

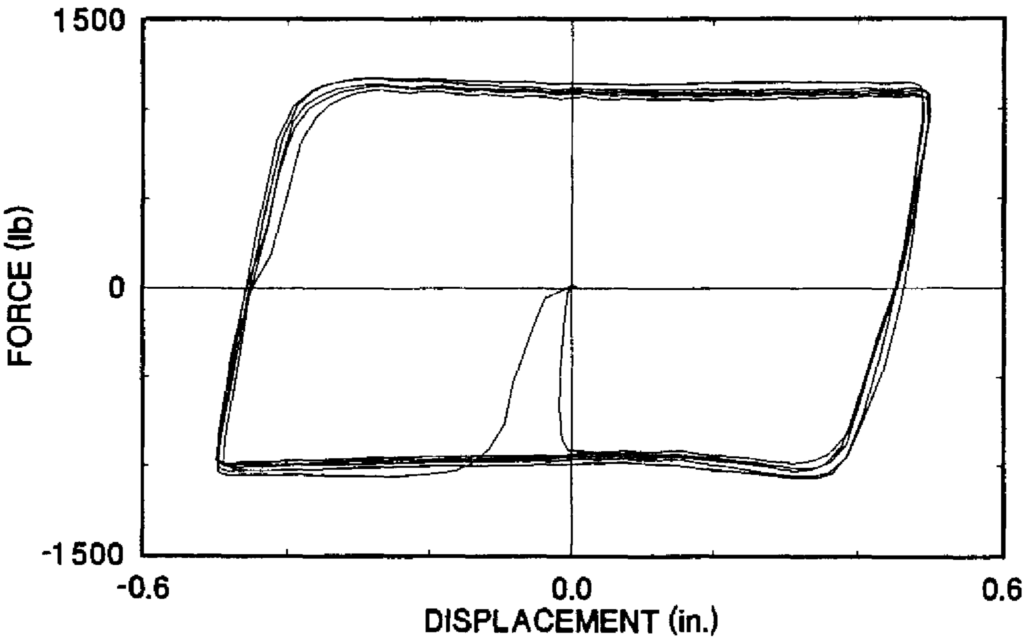

FIGURE 2-9 Recorded Force - Displacement Loop in Constant Velocity Test at Velocity of 12.6 in/sec and Temperature of 23°C (1 in. = 25.4 mm, 1 lb = 4.46 N)

property was obtained in additional tests with constant velocity motion (sawtooth displacement). Figure 2-9 shows the recorded force-displacement loop in one such test with amplitude of 0.5 in (12.7 mm) and constant velocity of 12.6 in/sec (320 mm/sec). Evidently, the output force is independent of amplitude.

Within the temperature range of about 0°C to 50°C, the device apparently exhibits a dependency of its mechanical properties on temperature. This dependency is discussed in detail in the next subsection. However, it is worthy of mentioning that this dependency is not significant. The reader may confirm in the results of Table 2-II (tests 16 to 20) that within the aforementioned range of temperatures, the loss stiffness of the damper reduces by a factor of less than 2. For comparison, viscoelastic material dampers exhibit a close to 50-fold decrease in about the same range of temperatures (see discussion in Section 1.3).

2.5 Mathematical Modeling

Over a large frequency range, the damper exhibits viscoelastic fluid behavior. The simplest model to account for this behavior is the Maxwell model (Bird 1987).

The Maxwell model is defined at the macroscopic level as

$$P + \lambda \dot{P} = C_o \dot{u} \qquad (2\text{-}13)$$

where λ is the relaxation time, and C_o is the damping constant at zero frequency. A more general Maxwell model may also be considered in which the derivatives are of fractional order (Makris 1991)

$$P + \lambda D^r[P] = C_o D^q[u] \qquad (2\text{-}14)$$

where $D^r[f(t)]$ is the fractional derivative of order r of the time dependent function f. For complex viscoelastic fluid behavior, Equation 2-14 may offer more control than Equation 2-13 in modeling the behavior.

The generalized Maxwell model was initially considered. The parameter q was set equal to unity based on the assumption that the damping coefficient of the device is independent of the velocity over a wide range of values. For $q = 1$, the parameter C_o becomes the damping constant at zero frequency. Parameters λ and r were then determined by curve fitting of experimental values of C and K_1 versus the frequency of motion. Analytical expressions for the mechanical properties are given by

$$K_1 = \frac{C_o \lambda \omega^{1+r} \sin(\frac{\pi r}{2})}{d} \tag{2-15}$$

$$C = \frac{K_2}{\omega} = \frac{C_o [1 + \lambda \omega^r \cos(\frac{\pi r}{2})]}{d} \tag{2-16}$$

$$d = 1 + \lambda^2 \omega^{2r} + 2\lambda \omega^r \cos(\frac{\pi r}{2}) \tag{2-17}$$

$$\delta = \tan^{-1}\left(\frac{K_2}{K_1}\right) \tag{2-18}$$

The calibration of the model of Equation 2-14 was performed for the case of room temperature, for which experimental data over a wide frequency range were available. The calibration resulted in parameters $r = 1$, $q = 1$, $\lambda = 0.006$ secs and $C_o = 88$ lb-sec/in (15.45 N-sec/mm). Interestingly, the calibrated model is the classical Maxwell model. A comparison of experimental and analytically derived properties of storage stiffness, damping coefficient and phase angle is presented in Figure 2-10. The comparison is very good except for frequencies above 20 Hz, where the model underpredicts the storage stiffness. Such frequencies are typically not considered in seismic analysis.

Furthermore, the model predicts nonzero storage stiffness in the low frequency range (< 2 Hz). The predicted storage stiffness is insignificant for practical purposes.

The damper exhibits a relaxation time of only 6 msec. This indicates that for low rates of damper force, the term $\lambda\dot{P}$ in Equation 2-13 is insignificant. This occurs for frequencies below a cutoff value of about 4 Hz. Accordingly, for typical structural applications the term $\lambda\dot{P}$ may be neglected. This will be confirmed in a subsequent section where shake table results are compared to analytical results.

The model of the damper below the cutoff frequency is simply

$$P = C_o \dot{u} \qquad (2\text{-}19)$$

and, thus, for most practical purposes the damper behaves as a linear viscous dashpot.

The effect that temperature has on the single parameter of the model, C_o, is investigated in Figure 2-11. The recorded peak force in each test is plotted against the imposed peak velocity for the three values of temperature. It may be seen that the experimental results may be fitted with straight lines with slope equal to C_o.

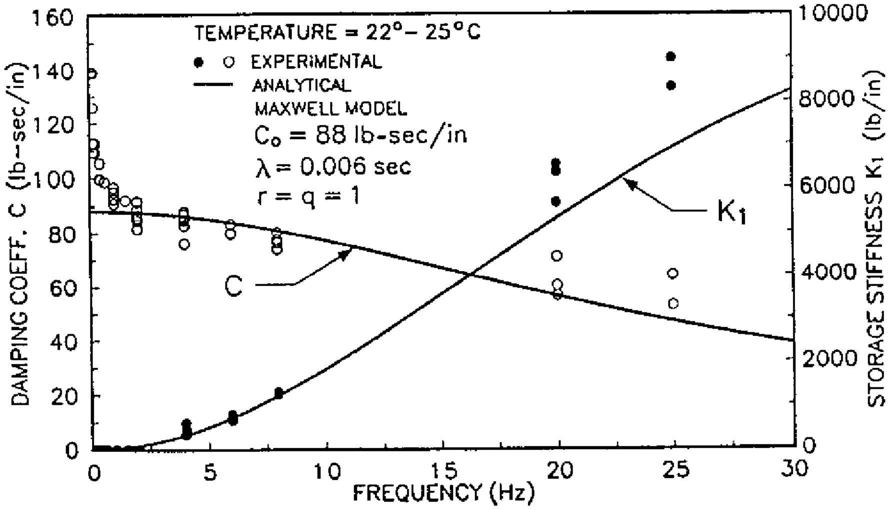

(a)

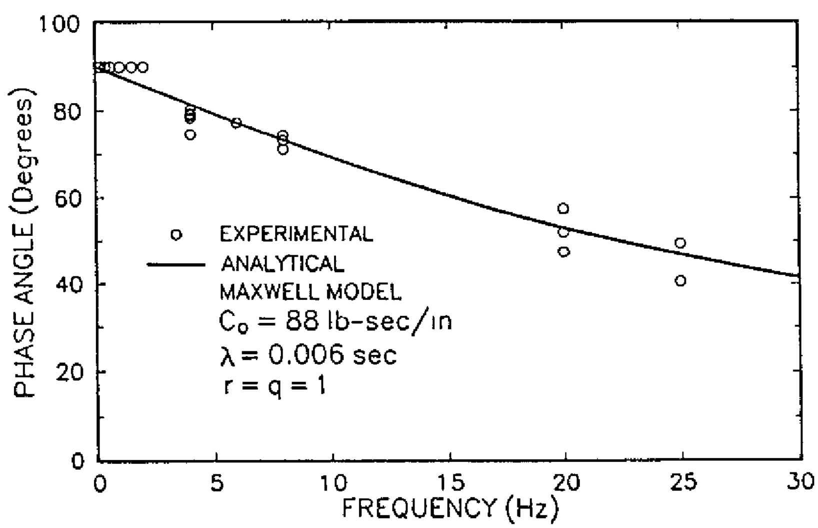

(b)

FIGURE 2-10 Comparison of Experimental and Analytically Derived Values of (a) Storage Stiffness and Damping Coefficient at Room Temperature and (b) Phase Angle at Room Temperature (1 in. = 25.4 mm, 1 lb = 4.46 N)

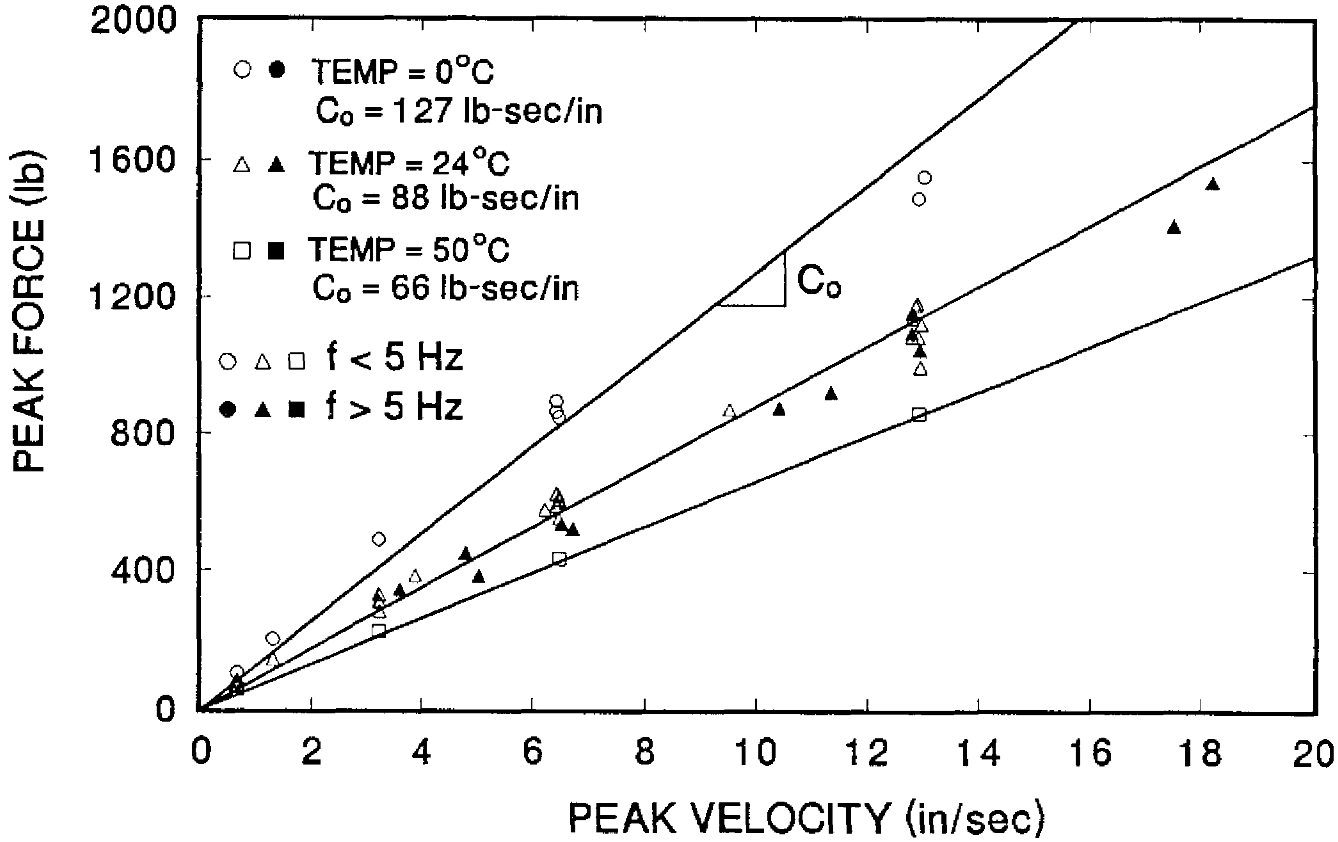

FIGURE 2-11 Recorded Values of Peak Force Versus Peak Velocity for Low, Room and High Temperature Tests (1 in. = 25.4 mm, 1 lb = 4.46 N)

For room temperature (24°C) and above, the behavior is indeed linear viscous to velocities of about 20 in/sec (508 mm/sec) and beyond. As temperature drops, the experimental results deviate from linearity at a lower velocity.

The values of constant C_o in Figure 2-11 demonstrate that the damper exhibits a stable behavior over a wide range of temperatures. Between about 0°C and 50°C, constant C_o reduces by a factor of less than 2. Assuming that a design for a building application will be anchored at a temperature of about 24°C, variations of temperature in the range of 0°C to 50°C will result in variations of the damping ratio of +44% to -25%. That is, if a design calls for a damping ratio of 20% of critical, extreme temperature variations will alter the damping ratio in the range of 15% to 29% of critical.